Circular RNA expression profiling and the potential role of hsa_circ_0005379 in decreased ovarian reserve

PENGYU HUANG[1*], SUZHU CHEN[2*], JIANSHU CAI[3*], CAIHONG JIANG[4], BICHEN LIU[5], YUN FU[1] and DIANLIANG LIN[1]

[1]Fujian Provincial Human Sperm Bank, Fujian Maternity and Child Health Hospital, College of Clinical Medicine for Obstetrics and Gynecology and Pediatrics, Fujian Medical University, Fuzhou, Fujian 350001, P.R. China; [2]Center of Reproductive Medicine, Fujian Maternity and Child Health Hospital, College of Clinical Medicine for Obstetrics and Gynecology and Pediatrics, Fujian Medical University, Fuzhou, Fujian 350001, P.R. China; [3]Nursing Department, Sir Run Run Shaw Hospital, Zhejiang University School of Medicine, Hangzhou, Zhejiang 310000, P.R. China; [4]Department of Medical Ultrasonics, Fujian Maternity and Child Health Hospital, College of Clinical Medicine for Obstetrics and Gynecology and Pediatrics, Fujian Medical University, Fuzhou, Fujian 350001, P.R. China; [5]Department of Laboratory Medicine, Fujian Medical University Union Hospital, Fuzhou, Fujian 350001, P.R. China

Received November 1, 2024; Accepted August 19, 2025

DOI: 10.3892/etm.2025.12974

Abstract. Decreased ovarian reserve (DOR) refers to the decreased ability of the ovaries to produce eggs and the low quality of the follicles, which may lead to abnormal menstruation and infertility. However, the role of circular RNAs (circRNAs) in DOR remains poorly understood. Through circRNA sequencing, hsa_circ_0005379 was identified as the most significantly upregulated circRNA in the follicular fluid exosomes of patients with DOR. The present study aimed to characterize the circRNA expression profile and investigate the function of hsa_circ_0005379 in DOR. Exosomes were isolated from the follicular fluid of individuals with DOR and healthy controls, followed by sequencing using the Illumina HiSeq platform. Functional enrichment analysis, including Gene Ontology and Kyoto Encyclopedia of Genes and Genomes analysis, was performed on the differentially expressed circRNAs. To further validate the results, the expression of five circRNAs was assessed in follicular fluid via reverse transcription-quantitative PCR (RT-qPCR). A DOR cell model was established by treating KGN granulosa cells with cyclophosphamide (CTX). Cell viability was evaluated using a Cell Counting Kit-8 assay following CTX exposure. hsa_circ_0005379 was either overexpressed or knocked down in the CTX-treated cells, and the levels of cell apoptosis, reactive oxygen species (ROS), malondialdehyde (MDA) and superoxide dismutase (SOD) were analyzed by flow cytometry and biochemical assays. Eight differentially expressed circRNAs were identified in individuals with DOR compared with controls, including seven upregulated and one downregulated. RT-qPCR confirmed that the expression trends of hsa_circ_0000344, hsa_circ_0001126, hsa-circ_0005379, hsa_circ-0005777 and hsa_circ_0007509 aligned with those from the sequencing results. Furthermore, overexpression and knockdown of hsa_circ_0005379 in KGN cells was verified by RT-qPCR. Silencing hsa_circ_0005379 in CTX-treated KGN cells promoted cell viability and reduced apoptosis, accompanied by reduced ROS and MDA levels and enhanced SOD activity. Overexpression of hsa_circ_0005379 yielded the opposite results. Collectively, the results suggested that hsa_circ_0005379 played a key role in regulating cell viability and oxidative stress in CTX-treated granulosa cells.

Correspondence to: Professor Yun Fu or Professor Dianliang Lin, Fujian Provincial Human Sperm Bank, Fujian Maternity and Child Health Hospital, College of Clinical Medicine for Obstetrics and Gynecology and Pediatrics, Fujian Medical University, 18 Daoshan Road, Gulou, Fuzhou, Fujian 350001, P.R. China
E-mail: yunfu1994china@163.com
E-mail: dianlianlin@163.com

*Contributed equally

Key words: decreased ovarian reserve, exosome, circular RNAs, hsa_circ_0005379

Introduction

Ovarian reserve, reflecting the female reproductive capacity, refers to the quantity and quality of follicles at various developmental stages (1,2). A significant reduction in baseline antral follicle count (AFC) and anti-Müllerian hormone (AMH) levels, coupled with an elevation in basal follicle-stimulating hormone (FSH), indicates decreased ovarian reserve (DOR) (3). Women with DOR exhibit impaired ovarian function, manifested by suboptimal responses to ovarian stimulation, decreased oocyte retrieval and higher cycle cancellation rates, all contributing to a lowered probability of successful conception (4). The impact of DOR on fertility has become increasingly pronounced with the delay of reproductive age. The etiology of DOR is complex, involving age, genetics, immune factors and environmental exposures (5).

For example, Biallelic germline BRCA1 frameshift mutations associated with isolated DOR (6); Dehydroepiandrosterone regulates the balance of CD4+/CD8+ T cells to improve balance of CD4+/CD8+ T cells with DOR (7); A history of heavy smoking may increase risk of DOR (8). Despite advances, the precise molecular mechanisms underlying DOR remain incompletely understood, highlighting the need to unravel the molecular pathways implicated in DOR and identify potential therapeutic targets.

Small extracellular vesicles (referred to as exosomes in the present study) play a key role in intercellular communication by transferring diverse molecules, including proteins, nucleic acids and metabolites (9,10). Increasing evidence highlights their function as central mediators of extracellular signaling, with substantial implications for biological processes, such as insulin signaling, lipolysis and inflammation (11,12). Exosomes have been extensively studied in the context of female reproductive disorders (13), such as polycystic ovary syndrome (PCOS) (14,15), intrauterine adhesion (16), premature ovarian insufficiency (POI) (17) and premature ovarian failure (18). However, the expression of exosome-derived circular RNAs (circRNAs) in DOR follicles remains underexplored. Oxidative stress, caused by an imbalance between pro-oxidants, such as reactive oxygen species (ROS) and nitrogen species, and the body's antioxidant defenses, can result in cellular damage to DNA, proteins and lipids (19). This imbalance is a recognized contributor to fertility decline in both sexes (20) and plays a marked role in ovarian aging (21). Huang *et al* (22) observed a notable decrease in the oxidative stress marker glutathione in follicular fluid from individuals with DOR compared with that in healthy controls. Despite these observations on oxidative stress in DOR, the precise mechanisms by which circRNAs participate in regulation remain poorly understood and are the subject of ongoing research.

To the best of our knowledge, no previous studies have explored the alterations in exosomal circRNA profiles in the follicular fluid of individuals with DOR. The present study represents the first attempt to assess the variations in circRNA expression within exosomes from the follicular fluid of patients with DOR. The current study aimed to evaluate the influence of key differentially expressed circRNAs on granulosa cells in DOR in terms of cell viability and oxidative stress, in an effort to identify potential therapeutic targets for DOR.

Materials and methods

Clinical samples. In total, 6 women diagnosed with DOR and 6 age-matched control women (median age, 32 years; range, 31-34 years) were recruited from Fujian Maternity and Child Health Hospital (Fuzhou, China), with ethics approval granted by the Ethics Committee of Fujian Maternity and Child Health Hospital (approval no. 2023KYLLR01082). Controls were women who presented for a routine fertility check-up or preconception consultation and were found to have no significant infertility or known fertility issues. All participants provided written informed consent. All patients presented to the hospital between January 2020 and December 2020. The subjects met the diagnostic criteria for DOR based on AMH <1.1 ng/ml and AFC <5 on transvaginal ultrasound (23,24). Exclusion criteria included any history of medication affecting glucose or lipid metabolism, as well as known conditions that cause hormonal, metabolic and reproductive abnormalities, such as Cushing's syndrome, endometriosis, congenital adrenal hyperplasia or androgen-secreting tumors. Preovulatory follicular fluid was collected from participants during oocyte retrieval, and samples were subsequently stored at -80˚C for RNA extraction and exosome isolation. The clinical characteristics of patients with DOR were obtained from medical records.

Exosome isolation. To identify differentially expressed circRNAs in exosomes of individuals with DOR and normal controls, exosomes were isolated from the follicular fluid of both groups using ultracentrifugation, as previously described (25). In brief, 500 μl follicular fluid was centrifuged at 10,000 x g for 45 min at 4˚C. The supernatant was filtered through a 0.45-μm membrane, and the filtrate was collected and transferred to a new centrifuge tube. Ultracentrifugation was then performed at 100,000 x g for 70 min at 4˚C. After removal of the supernatant, the pellet was resuspended in ice-cold PBS. The sample was subjected to another round of ultracentrifugation at 100,000 x g for 70 min at 4˚C. The resulting precipitate was resuspended in 100 μl PBS. The isolated exosomes were stored at -80˚C for further analysis.

Exosome analysis. Exosome isolation quality was assessed by diluting the samples with PBS (w/v=1:100), followed by analysis using the NanoSight LM10 instrument (Malvern Instruments, Ltd.) according to the manufacturer's instructions. Size and concentration were quantified through the Nanoparticle Tracking Analysis 2.0 (NTA 2.0) software (Malvern Instruments, Ltd.).

Transmission electron microscopy (TEM). To examine the structural characteristics of the isolated exosomes, 10 μl exosome suspension was carefully placed onto a 300 mesh formvar/carbon-coated copper grid (MilliporeSigma). The exosomes were allowed to adsorb to the grid for 1 min at room temperature, after which excess liquid was removed to ensure optimal sample preparation. The adsorbed exosomes were then subjected to negative staining with 2.5% uranyl acetate for 5 min and embedded with 1% methyl cellulose (Sigma-Aldrich, Shanghai, China) on ice for 10 min. Following staining, the samples were air-dried for several minutes at room temperature. Finally, the exosomes were analyzed using TEM (FEI Tecnai 12; Philips Medical Systems B.V.) at a magnification of x60,000 to observe their structural features.

Western blot analysis. Total protein of samples was separated by radio-immunoprecipitation assay lysis buffer (Beyotime Institute of Biotechnology), and then quantified using the BCA Protein Assay Kit (Beyotime Institute of Biotechnology). A total of 20 μg protein from each isolated exosome sample and follicular fluid [negative control (NC)] were subjected to SDS-PAGE on 10% gels for protein separation. The separated proteins were then transferred onto PVDF membranes and incubated overnight in TBS-Tween (TBS-T) buffer, containing Tris (15 mM, pH 7.8), NaCl (100 mM), Tween-20 (0.5%), with

5% defatted dry milk at 4˚C. The membranes were subsequently incubated with primary antibodies against CD9 (1:1,000; cat. no. ab236630; Abcam) and CD63 (1:1,000; cat. no. A5271; ABclonal Biotech Co., Ltd.) in TBS-T buffer with 5% defatted dry milk for 3 h at 25˚C. After washing with TBS-T buffer, the membranes were incubated with HRP-conjugated secondary antibodies (goat anti-mouse/rabbit IgG; cat. nos. SA00001-1& SA00001-2; Proteintech Group, Inc.) at a 1:2,000 dilution for 1 h at 25˚C. Protein bands were visualized using an electrochemiluminescence detection system (Pierce ECL Western; Thermo Fisher Scientific, Inc.). All experiments were repeated at least three times to ensure the reliability and reproducibility of the results.

circRNA sequencing and analysis. circRNA sequencing was employed to identify differentially expressed circRNAs in follicular fluid exosomes between four DOR and four normal control samples, as previously described (26). A concentration ≥50 ng/μl was used for each sample, and the EVs concentration was determined by NTA software as the basis for standardization. Total RNA was extracted from exosomes using TRIzol® (cat. no. 155976018; Invitrogen; Thermo Fisher Scientific, Inc.) as per the manufacturer's protocol, with RNA quality assessed using the optical density $(OD)_{260}/OD_{280}$ ratio between 1.8 and 2.0, adhering to establish quality control standards. For library construction, RNA was processed with the TruSeq Stranded Total RNA library preparation kit (cat. no. 20020599; Illumina, Inc.). Post-preparation, library quality and quantity were evaluated using the Bioanalyzer 2100 system (Agilent Technologies, Inc.). The prepared library, at a concentration of 10 pM, was converted into single-stranded DNA, which was then captured and amplified *in situ* to form clusters (using a dilute NaOH for denaturation and then hybiridzation and extension in ~35 cycles). Sequencing was performed for 150 cycles in paired-end mode on the Illumina HiSeq4000 sequencer (Illumina, Inc.) with the HiSeq 3000/4000 SBS Kit (150 cycles) (cat. no. TG-410-1002; Illumina, Inc.), ensuring a Q30 quality score. Following trimming of 30 adapters with Cutadapt software (v3.4; National Bioinformatics Infrastructure Sweden) and removal of low-quality sequences, high-quality read fragments were used for circRNA analysis. High-quality reads were aligned using the STAR software (v2.5.1b; National Human Genome Research Institute of NIH), while circRNAs were identified and analyzed with the DCC program (v0.4.4; Karolinska Institutet), and annotation of the detected circRNAs was performed using the Circ2Traits (http://gyanxet-beta.com/circdb/) and circBase (https://www.circbase.org/) databases. Data normalization and differential expression analysis of circRNAs were conducted with the EdgeR software (v3.16.5; https://bioconductor.org/packages/edgeR), with circRNAs considered differentially expressed when fold change was ≥2.0 and P<0.05. Heatmaps and clustering of differentially expressed circRNAs were generated using the R ggplot2 package (v2.1.0; https://www.rdocumentation.org/packages/ggplot2/versions/2.1.0) (27). Functional predictions of circRNAs were performed through Gene Ontology (GO; https://geneontology.org/) and Kyoto Encyclopedia of Genes and Genomes (KEGG; https://www.kegg.jp/) analyses on the associated genes. These analyses were carried out using the Database for Annotation, Visualization and Integrated Discovery (https://david.ncifcrf.gov/home.jsp) (28). Terms with Benjamini-Hochberg-adjusted P<0.05 and containing ≥5 annotated genes were considered statistically significant. The raw data were uploaded to the National Centre for Biotechnology Information Sequence Read Archive database (BioProject accession no. PRJNA1191187).

Reverse transcription-quantitative PCR (RT-qPCR). Total RNA was extracted from the follicular fluid precipitate following centrifugation using TRIzol. RT of the RNA into cDNA was carried out using a PrimeScript™ RT reagent kit with gDNA Eraser (Perfect Real Time) (cat. no. RR047Q; Takara Biotechnology Co., Ltd.) according to the manufacturer's instructions. The resulting cDNA was subsequently amplified by qPCR, utilizing the AceQ Universal SYBR qPCR Master Mix (cat. no. Q511; Vazyme Biotech Co., Ltd.) and the ABI 7500 PCR system (cat. no. 4351104; Applied Biosystems; Thermo Fisher Scientific, Inc.). The amplification protocol included an initial denaturation step at 95˚C for 15 sec, followed by 45 cycles of amplification at 55-60˚C for 15 sec, and a final extension step at 72˚C for 15 sec. Relative RNA expression levels were calculated using the $2^{-\Delta\Delta Cq}$ method and using GAPDH as the reference gene (29). All reactions were performed in triplicate to ensure reliability and reproducibility of the results. The reference sequence accession nos. of circRNAs were derived from the circBank database (http://www.circbank.cn/#/home). The circBank IDs of hsa_circ_0000344, hsa_circ_0001126, hsa_circ_0005379, hsa_circ_0005777 and hsa_circ_0007509 are hsa_RSF1_0004200, hsa_PTPRA_0009800, hsa_GDI2_0006400, hsa_ARHGEF28_0005700 and hsa_PPP4R1_0010200, respectively. Primer sequences are provided in Table I.

Cell culture. The KGN ovarian granulosa cell line was obtained from Shanghai Fuheng Biotechnology Co., Ltd., and cultured in DMEM/F12 medium (cat. no. 11320033, Gibco; Thermo Fisher Scientific, Inc.) supplemented with 10% fetal bovine serum (HyClone; Cytiva) and 0.5% penicillin-streptomycin (Invitrogen; Thermo Fisher Scientific, Inc.). The cells were maintained in a 5% CO_2 atmosphere at 37˚C with 100% humidity. Cyclophosphamide (CTX; cat. no. HY-17420; MedChemExpress) may destroy the follicular pool, leading to primary ovarian insufficiency (30). To induce cell damage, CTX was administered at concentrations of 0, 10, 15, 20, 25 and 30 μM for 24 h at 37˚C. The NC was treated without CTX.

Cell transfection. To investigate the role of hsa_circ_0005379 in KGN cells, short hairpin (sh)-hsa_circ_0005379 and NC sh-circRNA(pLKO.1), as well as hsa_circ_0005379-overexpression (OE) and NC plasmids (pcDNA3.1) were synthesized by GeneChem, Inc. KGN cells were transfected for 5 h with the corresponding plasmids (500 μM) using Lipofectamine® 2000 reagent (Invitrogen; Thermo Fisher Scientific, Inc.) at room temperature according to the manufacturer's protocol, as previously described (31). The transfection efficiency was detected by RT-qPCR 48 h after transfection. All subsequent experiments were performed 48 h after transfection. The sequences of sh-hsa_circ_0005379 and NC are presented in Table II.

Table I. Primer sequences used in the present study.

Gene	Sequence (5'-3')
GAPDH	F: ACAGCAACAGGGTGGTGGAC
	R: TTTGAGGGTGCAGCGAACTT
hsa-circ-0000344	F: GCTTGGTGTATGTTGGTATCAGT
	R: GAAGGCAGGCAGTATGGTATC
hsa-circ-0001126	F: ACAAGAACAGCAAGCACCAAT
	R: GCATCATCCATTACCACTCAGT
hsa-circ-0005379	F: AGATCAACCGTGTTATGAAACCAT
	R: TTGCCATTCACTGACATTATACCT
hsa-circ-0005777	F: TTCGTGTGCTTCCAACTTGA
	R: CACTGGGACTGGTTTCTGTAG
hsa-circ-0007509	F: CGAAAGGCTTGTGCTGAATG
	R: TCCAGGGCTGAAGGTATAATAATC

F, forward, R, reverse.

Table II. Sequence of shRNAs and scramble control.

Name	Sequence (5'-3')
hsa-circ-0005379-sh1	CTGTTGTGCTGACCTCTGA
hsa-circ-0005379-sh2	GACAGCTTCATGGTCCAGA
hsa-circ-0005379-sh3	TACCAGGATGTGCTGGTCA
sh-hsa-circ-0005379-NC	CCTAAGGTTAAGTCGCCCTCG

sh, short hairpin; NC, negative control.

Cell viability assay. Cell viability was assessed using Cell Counting Kit-8 (CCK-8) (cat. no. A311; Vazyme Biotech Co., Ltd.) according to the manufacturer's instructions, as previously described (32). Briefly, 10 μl CCK-8 reagent were added to each well of a 96-well plate ($3x10^3$ cells/well), followed by incubation for 1 h at 37˚C. Absorbance at 450 nm was measured using a BioTek multifunctional microplate reader (Agilent Technologies, Inc.).

Cell apoptosis assay. A total of $1x10^6$ cells were collected in the logarithmic phase, washed with PBS and then digested with trypsin (cat. no. C0205; Beyotime Institute of Biotechnology). After treatment with 30 μM CTX, $1x10^5$ KGN cells were incubated with 5 μl Annexin V-APC and 5 μl PI at room temperature for 15 min as per the manufacturer's instructions (Beyotime Institute of Biotechnology). The apoptosis rate was then evaluated by flow cytometry (FACSCalibur; BD Biosciences), and the data were analyzed utilizing FlowJo software (version 10.0.7; TreeStar, Inc.).

Biochemical assays of malondialdehyde (MDA) and superoxide dismutase (SOD). MDA and SOD levels of KGN cells were measured using the MDA detection kit (cat. no. A003-1) and SOD detection kit (cat. no. A001-3) from Nanjing Jiancheng Bioengineering Institute, following the manufacturer's protocols.

ROS detection. ROS detection was performed using a ROS detection kit (cat. no. MA0219; Dalian Meilun Biotechnology Co., Ltd.). KGN cells were seeded in a six-well plate and treated with 30 μM CTX for 24 h at room temperature. Each well received 1 ml dichlorodihydrofluorescein diacetate (DCFH-DA; prepared at a 1:1,000 dilution in basal DMEM/F12) and incubated at 37˚C for 20 min to allow probe uptake. Following incubation, the cells were washed with 1X PBS three times to remove excess probe. The cells were then digested with 0.25% Trypsin (cat. no. C0205; Beyotime Institute of Biotechnology), centrifuged at 300 x g for 5 min at 4˚C, and resuspended in 300 μl fresh ice-cold basal DMEM/F12 medium. ROS levels were quantified by flow cytometry (FACSCalibur; BD Biosciences), with excitation and emission wavelengths set at 488 nm and 525 nm, respectively, as previously described (33). The data were analyzed utilizing FlowJo software (version 10.0.7; TreeStar, Inc.). ROS mean fluorescence intensity ratio was calculated as the fluorescently stained cell number/total cell number.

Statistical analysis. All experiments were independently performed at least 3 times. Data are presented as the mean ± standard deviation and data analysis was performed using GraphPad Prism v9 software (GraphPad; Dotmatics). Comparisons between two groups were performed using unpaired Student's t-test. Comparisons among three or more groups were conducted using one-way ANOVA followed by Tukey's multiple comparisons test. $P<0.05$ was considered to indicate a statistically significant difference.

Results

Cohort characteristics and exosome characterization. The clinical characteristics of patients with DOR and controls were evaluated (Table III), and no significant differences in

Table III. General characteristics of the study population.

Characteristics	Normal control group	Decreased ovarian reserve group	P-value
Age, years	31.50±1.73	32.50±1.29	0.390
BMI	20.41±3.10	22.18±4.38	0.530
Duration of infertility, years	2.25±0.50	3.25±1.26	0.190
Estradiol baseline, pg/ml	31.25±10.71	44.25±13.45	0.180
Follicle-stimulating hormone baseline, mIU/ml	5.98±0.54	8.27±3.70	0.270
Luteinizing hormone baseline, mIU/ml	3.55±0.76	3.48±1.01	0.910
Anti-mullerian hormone baseline, ng/ml	3.91±0.71	0.73±0.23	<0.001
Antral follicle count	10.75±2.36	4.00±2.45	<0.010
Cleaved zygotes, %	91.25±12.74	82.50±13.58	0.380

Data are presented as the mean ± SD.

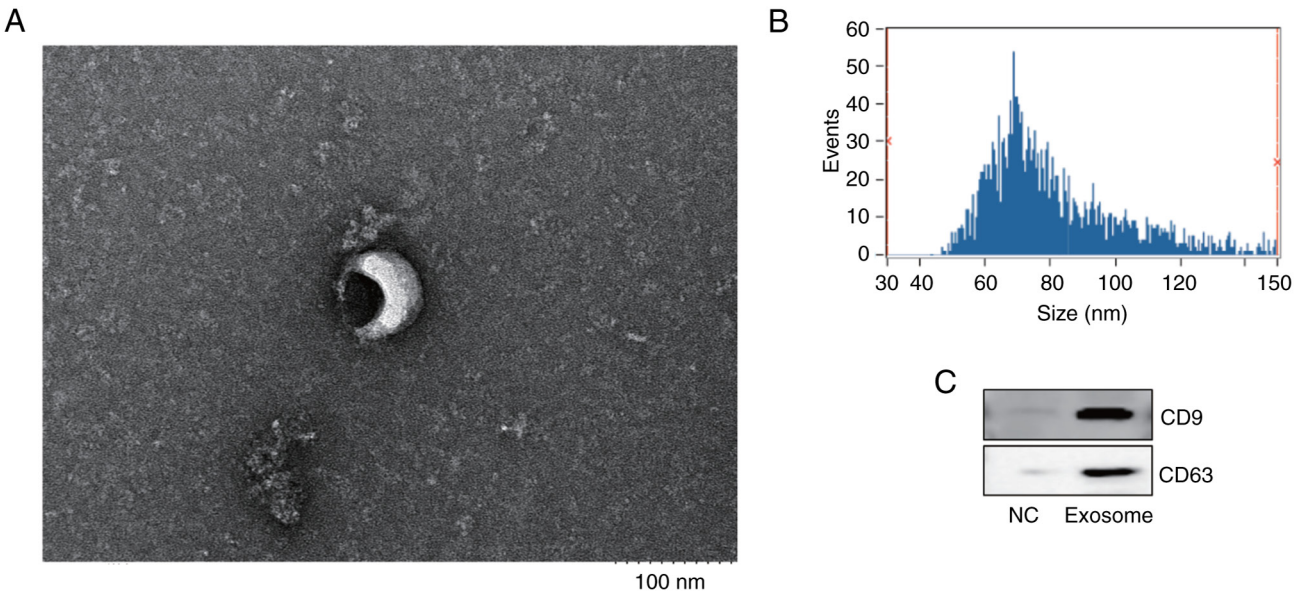

Figure 1. Characterization of the follicular fluid exosomes of patients with decreased ovarian reserve. (A) Representative transmission electron microscopy images of follicular fluid exosomes (magnification, x60,000). (B) The main range of size distribution of follicular fluid exosomes. (C) Western blot analysis of the exosome positive markers CD9 and CD63. The exosomes were from follicular fluid of DOR, and the negative control was the follicular fluid of DOR.

age, BMI, duration of infertility, estradiol, follicle-stimulating hormone, luteinizing hormone, anti-mullerian hormone and cleaved zygotes ratio between the two groups were observed. By contrast, significant differences in AMH and AFC levels between the DOR and control groups were detected. Significant decreases in AMH and AFC usually indicate a significant decline in ovarian reserve function, which may be accompanied by reduced fertility or an increased risk of menopausal-related conditions. Exosomes were then isolated from the follicular fluid of both DOR and control groups. TEM analysis was performed to examine exosome size and morphology (Fig. 1A). Nanoparticle tracking analysis determined the exosome size and concentration, revealing that the mean diameter was 81.18 nm and the concentration was $2.79x10^9$ particles/ml (Fig. 1B). Additionally, the presence of the exosome markers CD9 and CD63 was confirmed through western blot analysis of follicular fluid exosomes (Fig. 1C).

Expression profiling of circRNAs in patients with DOR. Differentially expressed circRNAs in exosomes were identified and summarized in Table IV. Information on the fold changes, P-values and the corresponding host genes of all eight circRNAs is provided. As illustrated in Fig. 2A, the volcano plot revealed a clear separation between the DOR and control groups, with seven circRNAs upregulated and one downregulated in the DOR group. The heatmap in Fig. 2B displays the expression profiles of these eight differentially expressed circRNAs.

Functional enrichment analysis. To explore the potential roles of differentially expressed circRNAs, GO and KEGG analyses were performed, focusing on the host genes associated with these circRNAs. The top 10 enriched terms related to molecular functions, cellular components and biological processes are summarized in Fig. 3A-C. The leading

Table IV. Differentially expressed circRNAs between patients with decreased ovarian reserve and normal controls.

circRNA ID	Log2 fold change	P-value	Host gene
hsa_circ_0000344	7.50	0.026802	RSF1
hsa_circ_0001126	6.95	0.040373	PTPRA
hsa_circ_0001068	6.66	0.049757	MGAT5
hsa_circ_0001359	6.88	0.042484	PHC3
hsa_circ_0004422	-6.90	0.041604	-
hsa_circ_0005379	8.49	0.012191	GDI2
hsa_circ_0005777	7.71	0.022859	RGNEF
hsa_circ_0007509	7.21	0.033397	PPP4R1

circRNA, circular RNA; -, unknown.

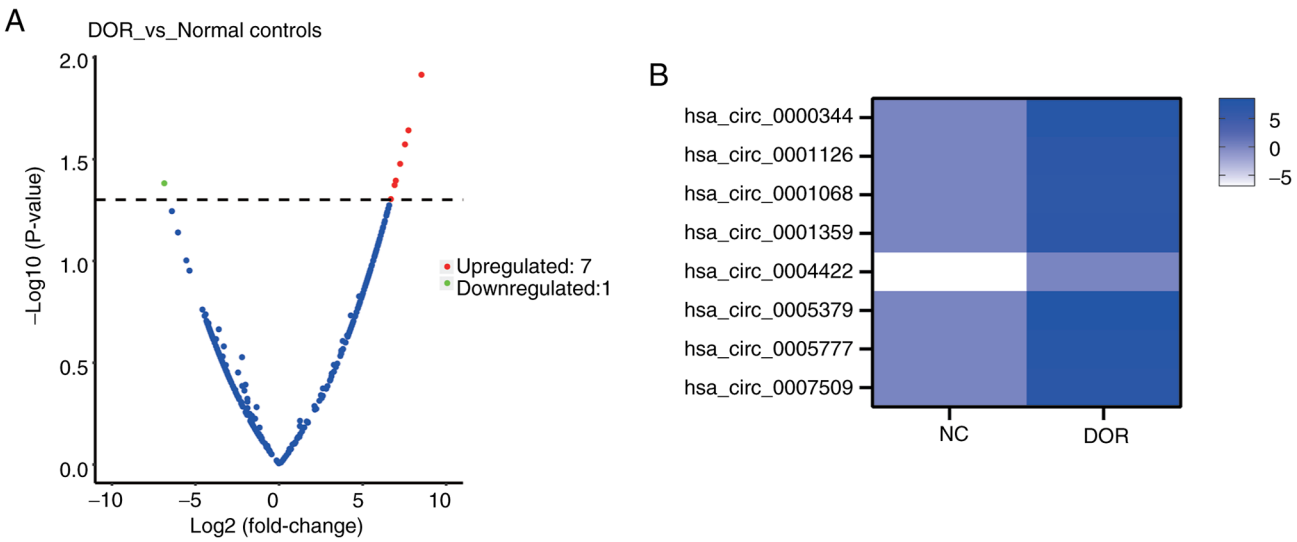

Figure 2. Differentially expressed circRNAs between patients with DOR and normal controls. (A) Volcano plots of all circRNAs. The red dots indicate upregulated circRNAs compared with normal controls, and the green dots indicate downregulated circRNAs compared with normal controls. (B) Heat map of differentially expressed circRNAs between patients with DOR and normal controls. The darker the color, the higher the relative expression level of circRNAs. NC, normal control; DOR, decreased ovarian reserve; circRNA, circular RNA.

biological processes included 'DNA-templated transcription, initiation' 'mitochondrial RNA 3'-end processing' and 'tRNA 3'-end processing' (Fig. 3A). For cellular components, the most enriched terms were 'NSL complex', 'ISWI-type complex' and 'PRC1 complex' (Fig. 3B). Regarding molecular functions, the most significant terms were 'GDP-dissociation inhibitor activity', 'histone acetyltransferase binding' and 'tRNA binding' (Fig. 3C). Additionally, five KEGG pathways were enriched (Fig. 3D), with the 'Notch signaling pathway' and 'Th1 and Th2 cell differentiation' showing significant enrichment ($P<0.05$), which suggests that these pathways may contribute to the pathogenesis of DOR.

Verification of selected circRNAs and the function of hsa_circ_0005379. In total, 6 patients with DOR and 6 normal controls were included for RT-qPCR validation. The top five most significantly altered genes, based on the P-value from the RNA-seq data, were selected for further validation (Table IV). Hsa_circ_0005379 was identified as the most significantly upregulated circRNA in the DOR group (Fig. 4) and was selected for subsequent analysis. Ovarian granulosa KGN cells were treated with varying concentrations of CTX (0, 10, 15, 20, 25 and 30 μM) to induce cellular damage. The CCK-8 assay demonstrated a dose-dependent decrease in KGN cell viability, with higher concentrations of CTX producing a more pronounced effect (Fig. 5A). The 30 μM CTX treatment was found to be the most effective in reducing cell viability. To further investigate the biological role of hsa_circ_0005379, it was selected as the optimal concentration for subsequent experiments. Then, KGN cells were transfected with shRNAs or an overexpression vector to explore the function of hsa_circ_0005379 (Fig. 5B and C). The results showed that sh1 had the highest knockdown efficiency and was therefore used for subsequent experiments (Fig. 5B). Following CTX treatment and transfection of the overexpression vector, a significant increase in the apoptosis rate was observed compared with that in CTX-treated KGN cells transfected with the NC vector. By contrast, knockdown of hsa_circ_0005379 with CTX treatment resulted in a decrease in apoptosis compared with sh-hsa_circ_0005379-NC+CTX group (Fig. 5D).

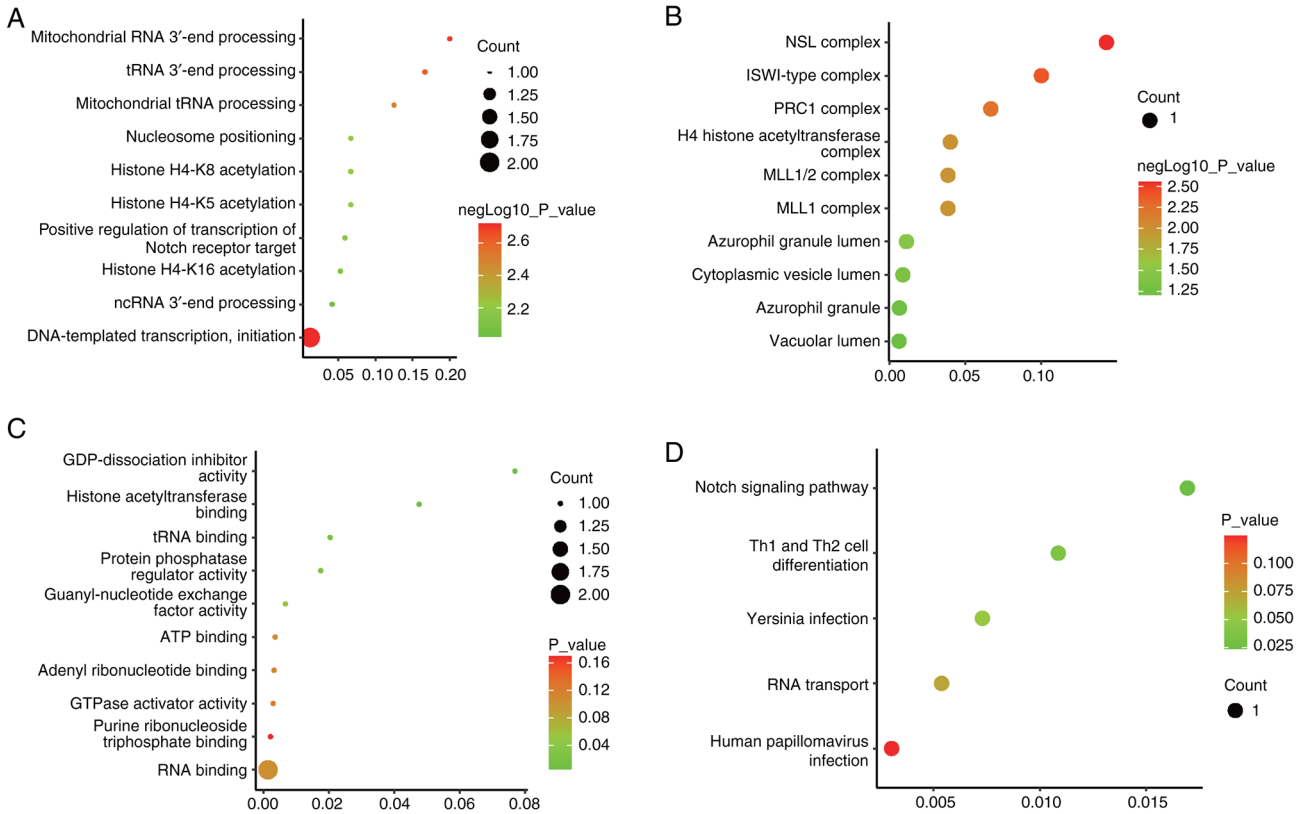

Figure 3. Functional analysis of differentially expressed circular RNA host genes. (A) Top 10 ranked biological process terms. (B) Top 10 ranked cellular component terms. (C) Top 10 ranked molecular function terms. (D) Enriched Kyoto Encyclopedia of Genes and Genomes pathways. NegLog10, negative logarithm 10.

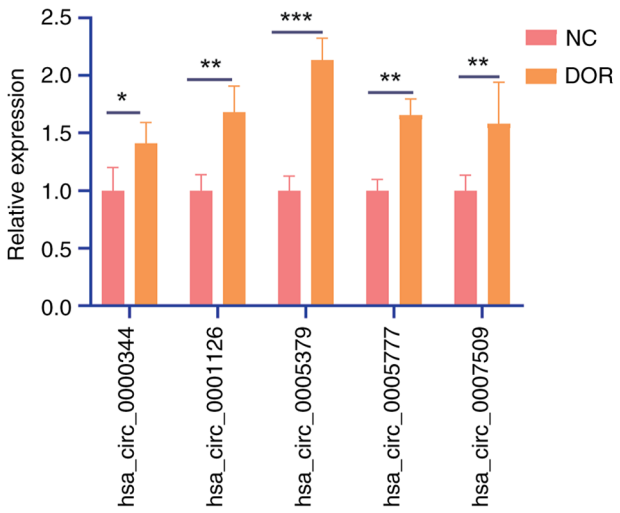

Figure 4. Reverse transcription-quantitative PCR analysis of the selected circular RNAs. Validation of hsa_circ_0000344, hsa_circ_0001126, hsa_circ_0005379, hsa_circ_0005777 and hsa_circ_0007509. n=6, *P<0.05, **P<0.01 and ***P<0.001. NC, normal control; DOR, decreased ovarian reserve.

The effect of hsa_circ_0005379 on oxidative stress in CTX-treated cells was further examined. The results indicated increased levels of ROS and MDA in the hsa_circ_0005379-OE group, whereas the sh-hsa_circ_0005379 group showed reduced levels of both markers, compared with those in the corresponding NC groups (Fig. 5E and F). By contrast, the antioxidant enzyme SOD, which is involved in aging processes, displayed an inverse pattern compared with that of ROS and MDA (Fig. 5G). These findings suggest that silencing hsa_circ_0005379 may alleviate oxidative stress in DOR.

Discussion

DOR is characterized by reduced oocyte quality and quantity, leading to impaired ovarian endocrine function and diminished fertility in women (34). The follicular microenvironment is believed to play a critical role in oocyte maturation and development (22). Therefore, the present study investigated the follicular microenvironment isolating exosomes (small vesicles containing biological molecules) from the follicular fluid of patients with DOR. A subsequent analysis of follicular exosomes using circRNA sequencing was performed, thus conducting the first examination of the exosomal circRNA profile in the follicular fluid of individuals with DOR, to the best of our knowledge.

circRNAs, a class of single-stranded RNA molecules, are characterized by covalently closed loops. These molecules are widely distributed across various organisms, ranging from viruses to mammals. Considerable progress has been made in understanding the biogenesis, regulation, localization, degradation and modification of circRNAs (35,36). In the present study, eight differentially expressed circRNAs were identified between patient with DOR and normal

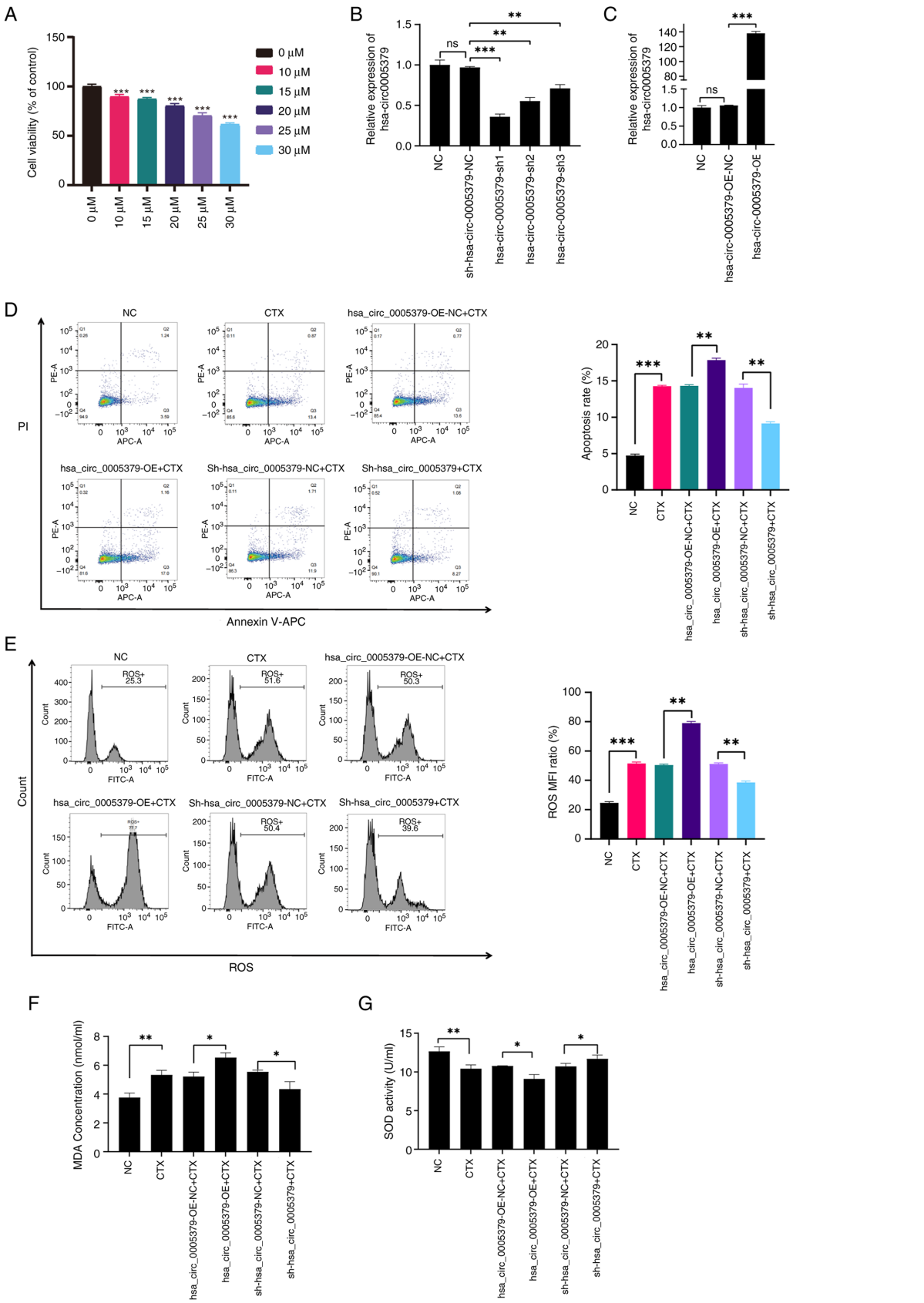

Figure 5. Function of hsa_circ_0005379 in CTX-induced KGN ovarian granulosa cells. (A) Different gradient concentrations (0, 10, 15, 20, 25 and 30 μM) of CTX were used to induce ovarian granulosa cell damage, and Cell Counting Kit-8 assay was used to detect KGN cell viability. (B) RT-qPCR analysis of hsa_circ_0005379 expression after transfection with three shRNAs and negative control sh-NC. (C) RT-qPCR analysis of hsa_circ_0005379 expression after transfection with OE vector and an empty OE-NC vector. (D) The apoptosis of sh-hsa_circ_0005379 or hsa_circ_0005379-OE transfected KGN cells was detected using annexin V/PI staining. (E) Flow cytometry was used to detect the ROS level of cells after different treatments. The concentration of (F) MDA and (G) SOD in KGN cells with different treatments was determined using corresponding biochemistry detection kits. n=3, *P<0.05, **P<0.01 and ***P<0.001 vs. 0 μM or as indicated. CTX, cyclophosphamide; RT-qPCR, reverse transcription-quantitative PCR; OE, overexpression; NC, negative control; sh, short hairpin; SOD, superoxide dismutase; MDA, malondialdehyde; ROS, reactive oxygen species; MFI, mean fluorescence intensity; ns, not significant.

controls, followed by enrichment analyses. GO biological process enrichment analysis revealed the involvement of the identified circRNAs in numerous biological processes, including 'DNA-templated transcription, initiation'. Notably, the enrichment of this process was also observed in rats with DOR, induced by tripterygium glycoside tablet suspension (37). Additionally, two key pathways were found to be significantly enriched: 'Notch signaling pathway' and 'Th1 and Th2 cell differentiation'. Hughes *et al* (38) reported that elevated ovarian oocyte death triggered an increase in Notch signaling and ovarian inflammation, and that Notch signaling pathway activation in granulosa cells exacerbated apoptosis. However, the specific role of the Notch pathway in DOR remains to be further elucidated. In addition, increased oxidative stress caused by smoking can further promote the onset and development of cancer by amplifying the inflammatory response and activating Notch-1 signaling (39). Overexpression of long non-coding RNA NONHSAT098487.2 has been shown to inhibit H_2O_2-induced oxidative stress injury in cardiomyocytes by activating Notch signaling pathway (40) and polystyrene microplastics have been demonstrated to promote colon barrier damage through oxidative stress-mediated overactivation of the Notch signaling pathway (41). These studies suggest an association between oxidative stress and Notch pathway activation. Since oxidative stress is closely related to DOR (42), future studies may explore the association between DOR and the Notch pathway in terms of oxidative stress generation. Furthermore, a recent study showed that polysaccharides could collectively inhibit inflammation, apoptosis and oxidative stress in asthmatic rats via regulation of T helper (Th)1/Th2 and Th17/Treg cell immune imbalances (43). Dehydroepiandrosterone has been shown to improve Th1 immune responses and regulate the balance of the Th1/Th2 response in patients with DOR (7). These studies collectively suggest that Th1/Th2 responses may be involved in the regulation of oxidative stress in DOR.

During follicular development, the interaction between oocytes and adjacent granulosa cells is essential for the production of fertilizable oocytes and the regulation of ovarian function (44-46). Thus, diminished oocyte competence in women with DOR may stem from dysregulated granulosa cell function (47). CTX exposure causes premature ovarian insufficiency (48). In the present study, a DOR cell model was established by exposing granulosa cells to CTX, and this model was subsequently used to investigate the role of hsa_circ_0005379.

Hsa_circ_0005379 has previously been identified as a key regulator in neuroblastoma (49). In the present study, upregulation of hsa_circ_0005379 was observed in exosomes isolated from the follicular fluid of patients with DOR. Silencing hsa_circ_0005379 partially reversed granulosa cell apoptosis. A significant association between oxidative stress and aging has been reported (50), with oxidative stress also being recognized as a major contributor to ovarian aging (21). Alterations in ROS, MDA and SOD levels reflect changes in oxidative stress, providing an indication of ovarian aging. Increased oxidative stress has been observed in both animal models and patients with DOR (22,51). In the present study, reduced hsa_circ_0005379 levels alleviated oxidative stress in CTX-induced DOR cells, suggesting the potential of hsa_circ_0005379 as a therapeutic target for DOR.

In addition, other circRNAs have been reported in the literature to be associated with DOR. For example, hsa_circ_0031584 has been indicated to be an important molecule regulating the mitotic process of granulosa cells in DOR (52). The findings of the present study were compared with studies on circRNAs in other female reproductive diseases, noting conserved roles in oxidative stress regulation. For example, Bu-Shen-Ning-Xin decoction has been shown to inhibit oxidative stress by regulating circRNA_012284 expression in POI. Human umbilical cord mesenchymal stem cell-derived exosomes secreted circBRCA1, which directly sponged microRNA (miR)-642a-5p to upregulate FOXO1, thereby preventing oxidative stress injuries in granulosa cells and protecting ovarian function in rats with POI (53). Furthermore, knockdown of hsa_circ_0118530 was shown to suppress PCOS progression by inhibiting oxidative stress and inflammation factor release (54). In another study, overexpression of circ_0097636 protected PCOS cell models from dihydrotestosterone-induced oxidative stress by increasing sirtuin 3 expression (55).

Hsa_circ_0005777 is derived from the cyclization of the host gene rho guanine nucleotide exchange factor (RGNEF); circRGNEF promotes bladder cancer progression via regulation of the miR-548/KIF2C axis (56). Similarly, hsa_circ_0001126 originates from the protein tyrosine phosphatase receptor type a (PTPRA) gene, and circPTPRA inhibits RNA N6-methyladenosine recognition by interacting with insulin-like growth factor 2 mRNA-binding protein 1, thereby suppressing bladder cancer progression (57). Future investigations involving small interfering RNA-mediated knockdown or overexpression of these circRNAs are essential to further elucidate their involvement in DOR pathogenesis.

The present study has certain limitations. The small sample size represents an important constraint in this pilot investigation. Due to the strict exclusion criteria (such as the lack of history of medications known to influence glucose and lipid metabolism) and the challenges in recruiting patients with well-defined DOR, achieving a larger cohort was logistically difficult within the study timeframe. In future studies, a multicenter collaboration is necessary to recruit a larger, more diverse cohort. Additionally, the exclusion of individuals with a history of medications affecting glucose or lipid metabolism, as well as conditions such as Cushing's syndrome, congenital adrenal hyperplasia, androgen-secreting tumors and endometriosis, is rooted in the need to minimize confounding variables. These factors could independently alter metabolic or hormonal outcomes under investigation, thereby obscuring the true effects of the intervention or exposure being studied. For example, medications influencing glucose/lipid metabolism (such as insulin, statins and glucocorticoids) could mask or exaggerate metabolic changes (58), compromising the assessment of the study's primary endpoints. Furthermore, endocrine disorders (such as Cushing's syndrome, congenital adrenal hyperplasia and androgen-secreting tumors) directly disrupt hormonal or metabolic pathways, potentially mimicking outcomes relevant to conditions like PCOS or insulin resistance (59-61). Endometriosis is known to alter follicular fluid composition and inflammatory pathways, which could independently influence the present study's

endpoints, such as ROS levels and associated pathways (20). By excluding these factors, the internal validity of the present study was enhanced, ensuring that the observed effects are more likely attributable to the variables under investigation rather than pre-existing conditions or treatments. Excluding certain groups of individuals bolsters confidence in causal inferences by reducing confounding factors, particularly in studies focusing on metabolic or endocrine mechanisms (such as studies evaluating insulin sensitivity or androgen levels). By contrast, the homogeneity of the study population may limit external validity. For instance, the results may not apply to individuals with overlapping conditions (such as patients with PCOS or untreated congenital adrenal hyperplasia) or those on common glucose/lipid-modifying therapies. This restricts the findings to a narrower, 'idealized' population. If the excluded conditions are rare (such as androgen-secreting tumors), their omission may not markedly impact applicability. As a preliminary study, the findings may be specific to idiopathic DOR. Future research should include stratified analyses comparing subgroups (patients with DOR with vs. without endometriosis) to evaluate the broader applicability of these results, consistent with a recent study on DOR heterogeneity (4).

In conclusion, the present study provided a comprehensive profile of circRNA expression in exosomes isolated from the follicular fluid of patients with DOR. Additionally, the current study represents, to the best of our knowledge, the first report on the role of hsa_circ_0005379 in DOR. The results demonstrated that silencing hsa_circ_0005379 alleviated apoptosis and oxidative stress in CTX-induced granulosa cells. However, the underlying mechanisms through which hsa_circ_0005379 modulates oxidative stress and contributes to DOR remain to be further explored.

Acknowledgements

Not applicable.

Funding

The present study was funded by the Fujian Natural Science Foundation (grant no. 2021J05083), the Joint Funds for the Innovation of Science and Technology of Fujian Province (grant no. 2023Y9384), the Fujian Provincial Health Technology Project (grant no. 2025QNGGA010) and the Zhejiang Medical and Health Project (grant no. 2023KY781).

Availability of data and materials

The raw RNA sequencing data generated in the present study may be found in the National Center for Biotechnology Information Sequence Read database under accession number PRJNA1191187 or at the following URL: https://www.ncbi.nlm.nih.gov/bioproject/?term=PRJNA1191187. The other data generated in the present study may be requested from the corresponding author.

Authors' contributions

PH, YF and DL were responsible for the conceptualization, design and execution of the study. PH, YF, JC and DL were responsible for drafting and revising the manuscript. SC, JC and CJ were responsible for resources and investigation. PH, SC, JC, CJ and BL analyzed and interpreted the data. SC and JC were responsible for reviewing and editing the manuscript. PH, YF and DL confirm the authenticity of all the raw data. All authors read and approved the final manuscript.

Ethics approval and consent to participate

The present study was approved by the Ethics Committee of Fujian Maternity and Child Health Hospital (approval no. 2023KYLLR01082; Fuzhou, China). Written informed consent was obtained from all participants.

Patient consent for publication

Not applicable.

Competing interests

The authors declare that they have no competing interests.

References

1. Rotshenker-Olshinka K, Michaeli J, Srebnik N, Samueloff A, Magen S, Farkash R and Eldar-Geva T: Extended fertility at highly advanced reproductive age is not related to anti-Mullerian hormone concentrations. Reprod Biomed Online 45: 147-152, 2022.
2. Wen J, Huang K, Du X, Zhang H, Ding T, Zhang C, Ma W, Zhong Y, Qu W, Liu Y, *et al*: Can Inhibin B Reflect ovarian reserve of healthy reproductive age women effectively? Front Endocrinol (Lausanne) 12: 626534, 2021.
3. Liang C, Zhang X, Qi C, Hu H, Zhang Q, Zhu X and Fu Y: UHPLC-MS-MS analysis of oxylipins metabolomics components of follicular fluid in infertile individuals with diminished ovarian reserve. Reprod Biol Endocrinol 19: 143, 2021.
4. Cedars MI: Managing poor ovarian response in the patient with diminished ovarian reserve. Fertil Steril 117: 655-656, 2022.
5. Park SU, Walsh L and Berkowitz KM: Mechanisms of ovarian aging. Reproduction 162: R19-R33, 2021.
6. Helbling-Leclerc A, Falampin M, Heddar A, Guerrini-Rousseau L, Marchand M, Cavadias I, Auger N, Bressac-de Paillerets B, Brugieres L, Lopez BS, *et al*: Biallelic Germline BRCA1 Frameshift mutations associated with isolated diminished ovarian reserve. Int J Mol Sci 25: 12460, 2024.
7. Zhang J, Qiu X, Gui Y, Xu Y, Li D and Wang L: Dehydroepiandrosterone improves the ovarian reserve of women with diminished ovarian reserve and is a potential regulator of the immune response in the ovaries. Biosci Trends 9: 350-359, 2015.
8. Oladipupo I, Ali T, Hein DW, Pagidas K, Bohler H, Doll MA, Mann ML, Gentry A, Chiang JL, Pierson RC, *et al*: Association between cigarette smoking and ovarian reserve among women seeking fertility care. PLoS One 17: e0278998, 2022.
9. Ma X, Chen Z, Chen W, Chen Z and Meng X: Exosome subpopulations: The isolation and the functions in diseases. Gene 893: 147905, 2023.
10. Gregory CD and Rimmer MP: Extracellular vesicles arising from apoptosis: Forms, functions, and applications. J Pathol 260: 592-608, 2023.
11. Quan M and Kuang S: Exosomal secretion of adipose tissue during various physiological states. Pharmaceutical Res 37: 221, 2020.
12. Gallet R, Dawkins J, Valle J, Simsolo E, de Couto G, Middleton R, Tseliou E, Luthringer D, Kreke M, Smith RR, *et al*: Exosomes secreted by cardiosphere-derived cells reduce scarring, attenuate adverse remodelling, and improve function in acute and chronic porcine myocardial infarction. Eur Heart J 38: 201-211, 2017.
13. Esfandyari S, Elkafas H, Chugh RM, Park HS, Navarro A and Al-Hendy A: Exosomes as biomarkers for female reproductive diseases diagnosis and therapy. Int J Mol Sci 22: 2165, 2021.

14. Yuan D, Luo J, Sun Y, Hao L, Zheng J and Yang Z: PCOS follicular fluid derived exosomal miR-424-5p induces granulosa cells senescence by targeting CDCA4 expression. Cell Signal 85: 110030, 2021.
15. Cao J, Huo P, Cui K, Wei H, Cao J, Wang J, Liu Q, Lei X and Zhang S: Follicular fluid-derived exosomal miR-143-3p/miR-155-5p regulate follicular dysplasia by modulating glycolysis in granulosa cells in polycystic ovary syndrome. Cell Commun Signal 20: 61, 2022.
16. Yao Y, Chen R, Wang G, Zhang Y and Liu F: Exosomes derived from mesenchymal stem cells reverse EMT via TGF-beta1/Smad pathway and promote repair of damaged endometrium. Stem Cell Res Ther 10: 225, 2019.
17. Li Z, Zhang M, Zheng J, Tian Y, Zhang H, Tan Y, Li Q, Zhang J and Huang X: Human umbilical cord mesenchymal stem cell-derived exosomes improve ovarian function and proliferation of premature ovarian insufficiency by regulating the hippo signaling pathway. Front Endocrinol (Lausanne) 12: 711902, 2021.
18. Qu Q, Liu L, Cui Y, Liu H, Yi J, Bing W, Liu C, Jiang D and Bi Y: miR-126-3p containing exosomes derived from human umbilical cord mesenchymal stem cells promote angiogenesis and attenuate ovarian granulosa cell apoptosis in a preclinical rat model of premature ovarian failure. Stem Cell Res Ther 13: 352, 2022.
19. Burton GJ and Jauniaux E: Oxidative stress. Best Pract Res Clin Obstet Gynaecol 25: 287-299, 2011.
20. Agarwal A, Aponte-Mellado A, Premkumar BJ, Shaman A and Gupta S: The effects of oxidative stress on female reproduction: A review. Reprod Biol Endocrinol 10: 49, 2012.
21. Wang L, Tang J, Wang L, Tan F, Song H, Zhou J and Li F: Oxidative stress in oocyte aging and female reproduction. J Cell Physiol 236: 7966-7983, 2021.
22. Huang Y, Cheng Y, Zhang M, Xia Y, Chen X, Xian Y, Lin D, Xie S and Guo X: Oxidative stress and inflammatory markers in ovarian follicular fluid of women with diminished ovarian reserve during in vitro fertilization. J Ovarian Res 16: 206, 2023.
23. Zhang Q, Zhang D, Liu H, Fu J, Tang L and Rao M: Associations between a normal-range free thyroxine concentration and ovarian reserve in infertile women undergoing treatment via assisted reproductive technology. Reprod Biol Endocrinol 22: 72, 2024.
24. Can S, Yang X, He Y, Wang C, Zou H, Fan Q, Xu X, Cai G, Yunxia C and Xiaoqing P: Diminished ovarian reserve associates with pregnancy and birth outcomes after IVF: A retrospective cohort study. Hum Fertil (Camb) 27: 2414813, 2024.
25. Lin Q, Qi Q, Hou S, Chen Z, Jiang N, Zhang L and Lin C: Exosomal circular RNA hsa_circ_007293 promotes proliferation, migration, invasion, and epithelial-mesenchymal transition of papillary thyroid carcinoma cells through regulation of the microRNA-653-5p/paired box 6 axis. Bioengineered 12: 10136-10149, 2021.
26. Xiong S, Peng H, Ding X, Wang X, Wang L, Wu C, Wang S, Xu H and Liu Y: Circular RNA expression profiling and the potential role of hsa_circ_0089172 in Hashimoto's thyroiditis via sponging miR125a-3p. Mol Ther Nucleic Acids 17: 38-48, 2019.
27. Gustavsson EK, Zhang D, Reynolds RH, Garcia-Ruiz S and Ryten M: ggtranscript: An R package for the visualization and interpretation of transcript isoforms using ggplot2. Bioinformatics 38: 3844-3846, 2022.
28. Sherman BT, Hao M, Qiu J, Jiao X, Baseler MW, Lane HC, Imamichi T and Chang W: DAVID: A web server for functional enrichment analysis and functional annotation of gene lists (2021 update). Nucleic Acids Res 50: W216-W221, 2022.
29. Livak KJ and Schmittgen TD: Analysis of relative gene expression data using real-time quantitative PCR and the 2(-Delta Delta C(T)) method. Methods 25: 402-408, 2001.
30. Kalich-Philosoph L, Roness H, Carmely A, Fishel-Bartal M, Ligumsky H, Paglin S, Wolf I, Kanety H, Sredni B and Meirow D: Cyclophosphamide triggers follicle activation and 'burnout'; AS101 prevents follicle loss and preserves fertility. Sci Transl Med 5: 185ra62, 2013.
31. Mao X, Meng Q, Han J, Shen L, Sui X, Gu Y and Wu G: Regulation of dynamin-related protein 1 (DRP1) levels modulates myoblast atrophy induced by C26 colon cancer-conditioned medium. Transl Cancer Res 10: 3020-3032, 2021.
32. Zhang D, Yi S, Cai B, Wang Z, Chen M, Zheng Z and Zhou C: Involvement of ferroptosis in the granulosa cells proliferation of PCOS through the circRHBG/miR-515/SLC7A11 axis. Ann Transl Med 9: 1348, 2021.
33. Sun L, Wang H, Yu S, Zhang L, Jiang J and Zhou Q: Herceptin induces ferroptosis and mitochondrial dysfunction in H9c2 cells. Int J Mol Med 49: 17, 2022.
34. Lv Z, Lv Z, Song L, Zhang Q and Zhu S: Role of lncRNAs in the pathogenic mechanism of human decreased ovarian reserve. Front Genet 14: 1056061, 2023.
35. Zhou WY, Cai ZR, Liu J, Wang DS, Ju HQ and Xu RH: Circular RNA: metabolism, functions and interactions with proteins. Mol Cancer 19: 172, 2020.
36. Patop IL, Wust S and Kadener S: Past, present, and future of circRNAs. EMBO J 38: e100836, 2019.
37. Lu G, Zhu YY, Li HX, Yin YL, Shen J and Shen MH: Effects of acupuncture treatment on microRNAs expression in ovarian tissues from Tripterygium glycoside-induced diminished ovarian reserve rats. Front Genet 13: 968711, 2022.
38. Hughes CHK, Smith OE, Meinsohn MC, Brunelle M, Gevry N and Murphy BD: Steroidogenic factor 1 (SF-1; Nr5a1) regulates the formation of the ovarian reserve. Proc Natl Acad Sci USA 120: e2220849120, 2023.
39. Chiappara G, Di Vincenzo S, Cascio C and Pace E: Stem cells, Notch-1 signaling, and oxidative stress: A hellish trio in cancer development and progression within the airways. Is there a role for natural compounds? Carcinogenesis 45: 621-629, 2024.
40. Feng G, Zhang H, Guo Q, Shen X, Wang S, Guo Y and Zhong X: NONHSAT098487.2 protects cardiomyocytes from oxidative stress injury by regulating the Notch pathway. Heliyon 9: e17388, 2023.
41. Shaoyong W, Jin H, Jiang X, Xu B, Liu Y, Wang Y and Jin M: Benzo [a] pyrene-loaded aged polystyrene microplastics promote colonic barrier injury via oxidative stress-mediated notch signalling. J Hazard Mater 457: 131820, 2023.
42. Zhou Z, Li Y, Ding J, Sun S, Cheng W, Yu J, Cai Z, Ni Z and Yu C: Chronic unpredictable stress induces anxiety-like behavior and oxidative stress, leading to diminished ovarian reserve. Sci Rep 14: 30681, 2024.
43. Zhang B, Zeng M, Zhang Q, Wang R, Jia J, Cao B, Liu M, Guo P, Zhang Y, Zheng X and Feng W: Ephedrae Herba polysaccharides inhibit the inflammation of ovalbumin induced asthma by regulating Th1/Th2 and Th17/Treg cell immune imbalance. Mol Immunol 152: 14-26, 2022.
44. Buratini J, Dellaqua TT, Dal Canto M, La Marca A, Carone D, Mignini Renzini M and Webb R: The putative roles of FSH and AMH in the regulation of oocyte developmental competence: From fertility prognosis to mechanisms underlying age-related subfertility. Hum Reprod Update 28: 232-254, 2022.
45. Gilchrist RB, Lane M and Thompson JG: Oocyte-secreted factors: Regulators of cumulus cell function and oocyte quality. Hum Reprod Update 14: 159-177, 2008.
46. Jin L, Yang Q, Zhou C, Liu L, Wang H, Hou M, Wu Y, Shi F, Sheng J and Huang H: Profiles for long non-coding RNAs in ovarian granulosa cells from women with PCOS with or without hyperandrogenism. Reprod Biomed Online 37: 613-623, 2018.
47. Levi AJ, Raynault MF, Bergh PA, Drews MR, Miller BT and Scott RT Jr: Reproductive outcome in patients with diminished ovarian reserve. Fertil Steril 76: 666-669, 2001.
48. Zhang S, Zou X, Feng X, Shi S, Zheng Y, Li Q and Wu Y: Exosomes derived from hypoxic mesenchymal stem cell ameliorate premature ovarian insufficiency by reducing mitochondrial oxidative stress. Sci Rep 15: 8235, 2025.
49. Zhang L, Zhou H, Li J, Wang X, Zhang X, Shi T and Feng G: Comprehensive Characterization of Circular RNAs in Neuroblastoma Cell Lines. Technol Cancer Res Treat 19: 1533033820957622, 2020.
50. Khan F, Chen Y, Hartwell HJ, Yan J, Lin YH, Freedman A, Zhang Z, Zhang Y, Lambe AT, Turpin BJ, *et al*: Heterogeneous oxidation products of fine particulate isoprene Epoxydiol-derived methyltetrol sulfates increase oxidative stress and inflammatory gene responses in human lung cells. Chem Res Toxicol 36: 1814-1825, 2023.
51. Li F, Wang Y, Xu M, Hu N, Miao J, Zhao Y and Wang L: Single-nucleus RNA Sequencing reveals the mechanism of cigarette smoke exposure on diminished ovarian reserve in mice. Ecotoxicol Environ Saf 245: 114093, 2022.
52. Chen P, Li W, Liu X, Wang Y, Mai H and Huang R: Circular RNA expression profiles of ovarian granulosa cells in advanced-age women explain new mechanisms of ovarian aging. Epigenomics 14: 1029-1038, 2022.

53. Zhu X, Li W, Lu M, Shang J, Zhou J, Lin L, Liu Y, Xing J, Zhang M, Zhao S, *et al*: M^{6}A demethylase FTO-stabilized exosomal circBRCA1 alleviates oxidative stress-induced granulosa cell damage via the miR-642a-5p/FOXO1 axis. J Nanobiotechnology 22: 367, 2024.
54. Jia C, Wang S, Yin C, Liu L, Zhou L and Ma Y: Loss of hsa_circ_0118530 inhibits human Granulosa-like tumor cell line KGN cell injury by sponging miR-136. Gene 744: 144591, 2020.
55. Wang S, Wang Y, Qin Q, Li J, Chen Q, Zhang Y, Li X and Liu J: Berberine protects against Dihydrotestosterone-induced human ovarian granulosa cell injury and ferroptosis by regulating the circ_0097636/MiR-186-5p/SIRT3 pathway. Appl Biochem Biotechnol 196: 5265-5282, 2024.
56. Yang C, Li Q, Chen X, Zhang Z, Mou Z, Ye F, Jin S, Jun X, Tang F and Jiang H: Circular RNA circRGNEF promotes bladder cancer progression via miR-548/KIF2C axis regulation. Aging (Albany NY) 12: 6865-6879, 2020.
57. Xie F, Huang C, Liu F, Zhang H, Xiao X, Sun J, Zhang X and Jiang G: CircPTPRA blocks the recognition of RNA N^6-methyladenosine through interacting with IGF2BP1 to suppress bladder cancer progression. Mol Cancer 20: 68, 2021.
58. She J, Tuerhongjiang G, Guo M, Liu J, Hao X, Guo L, Liu N, Xi W, Zheng T, Du B, *et al*: Statins aggravate insulin resistance through reduced blood glucagon-like peptide-1 levels in a microbiota-dependent manner. Cell Metab 36: 408-421.e5, 2024.
59. Ferriere A and Tabarin A: Cushing's syndrome: Treatment and new therapeutic approaches. Best Pract Res Clin Endocrinol Metab 34: 101381, 2020.
60. Auer MK, Nordenstrom A, Lajic S and Reisch N: Congenital adrenal hyperplasia. Lancet 401: 227-244, 2023.
61. Macut D, Ilic D, Mitrovic Jovanovic A and Bjekic-Macut J: Androgen-Secreting ovarian tumors. Front Horm Res 53: 100-107, 2019.